한국기계가공학회지, 제19권, 제10호, pp. 8～15(2020.10) ISSN 1598-6721(Print)
Journal of the Korean Society of Manufacturing Process Engineers, Vol. 19, No. 10, pp. 8~15(2020.10) ISSN 2288-0771(Online)

https://doi.org/10.14775/ksmpe.2020.19.10.008

Multifunctional Transdermal Diffusion Test System

Mengyan Gao[*], Hu Jin[**], Xiang Fan Piao[*,#]

[*]Department of Electronic Information Engineering., Yanbian University
[**]Ganting Network Technology Co., Ltd. Shanghai

다기능 경피 확산 테스트 시스템 설계 및 제작

고멍얀*, 김호, 박상범*,#**

[*]연변대학교 공학원 전자정보학과, [**]간팅인너넷기술, 상해

(Received 04 July 2020; received in revised form 16 July 2020; accepted 19 July 2020)

ABSTRACT

The diffusion cell method is the main technique employed for the in vitro diffusion test of transdermal drug delivery preparations. Most existing transdermal diffusion devices use a water bath heating structure and direct current motor magnetic stirrer. However, these devices are confronted with problems, such as large volume, incompatible vertical and horizontal diffusion cells, few diffusion cell sets, and poor reliability. To overcome these deficiencies, the system adopts a dry heating method and uses a rotating magnetic field generated by the electromagnetic stirrer to drive the magnetic stirrer. Accordingly, the resulting device is characterized by a simple structure and small volume, convenient operation, compatible vertical and horizontal diffusion cells, and numerous diffusion cell sets. The reliability and practicability of the system is verified by the in vitro percutaneous permeability test of the bisoprolol patch.

Keywords : Transdermal Diffuser(경피 디퓨져), Electromagnetic Stirring(전자기 교반), MCU(마이크로 프로세스)

1. Introduction

With the scientific and technological advancements in the treatment of diseases, choosing a painless, convenient, and effective treatment method has increasingly become a popular option. Transdermal drug delivery refers to the use of a drug patch (a patch containing drugs and capable of controlling the delivery process) pasted on the surface of the skin, allowing the drug molecules to penetrate the skin surface. The molecules pass through the epidermis and dermis layers, and reach the subcutaneous tissue. After the drug is absorbed through the lymphatic vessels and capillaries, it eventually enters the human circulatory system to achieve the purpose of treatment[1]. Transdermal absorption must be observed in a simulated in vivo environment before new transdermal drugs are released into the market; accordingly, the diffusion cell method[2] is adopted to conduct transdermal test research. Among the parameters obtained, the most important evaluation criterion is the transdermal coefficient[3]. The traditional Franz diffusion cell[4]

Corresponding Author : pxf@ybu.edu.cn
Tel: +86-273-2243, Fax: +86-273-2243

(including the K–C diffusion cell[5] improved by Keshary et al.) and V–C diffusion cell have complex structures and few experimental sets. A magnetic stirrer is usually employed in the stirring method, and each diffusion cell has to be equipped with a set of magnetic stirring devices. The stirring motor adopts a direct current (DC) brush motor, and heating is afforded through the circulation of warm water. The volume of such a device is large, and its service life is short; both are not suitable for the microminiaturization of the instrument. Hence, the fabrication of this device cannot satisfy the requirements of experimentation on humans. In contrast, a multifunctional transdermal diffusion test system adopts a dry heating method and utilizes a rotating magnetic field generated by the electromagnetic stirrer to drive the magnetic stirrer. As a result, the test system is characterized by a simple structure and small volume, convenient operation, compatible vertical and horizontal diffusion cells, and numerous diffusion cells. The improved diffusion cell has a smaller volume and a large effective diffusion area. The inner diameter of the sampling port is expanded to 8 mm, and the 1-mL pipette tip can be directly inserted, making sampling less exhausting and considerably convenient. The use of steel chip clips reduces the volume.

The heater temperature, stirring speed, sampling timetable, and sampling time are displayed on the touchscreen. The temperature control range is 30–45 °C, and the electromagnetic stirring speed range is 350–800 rpm. The number of sampling alarm points is 20, and the set range for each sampling period is 0–99 h.

2. System Structure and Working Principle

2.1 Overall Structure

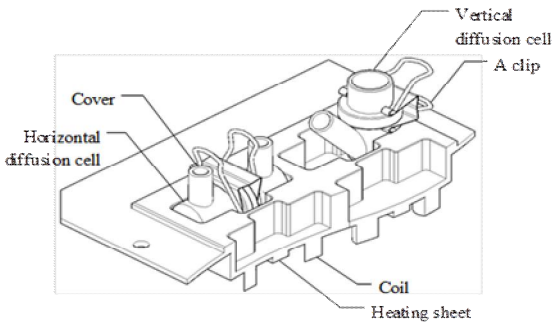

Fig. 1 Heater planning

Fig. 2 Physical diagram of diffusion test system

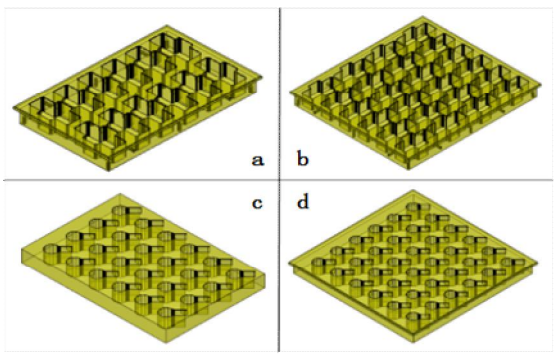

Fig. 3 Design drawing of heating plate

The multifunctional in vitro transdermal diffusion test device includes vertical diffusion cells, horizontal diffusion cells, steel clips, dry heaters, electromagnetic stirring coils group, and control circuits. The heater is composed of an aluminum alloy heating plate, alumina oxide ceramic heating plate, a temperature sensor, etc.

The plan view of the heater is shown in Fig. 1; the horizontal diffusion cell is shown on the left,

and the vertical diffusion cell is on the right. The bottom of the heating plate is provided with oxidized ceramic heating sheets, coils, and temperature sensors. A heating plate with a size of 70 × 10 × 10 mm was affixed to the hot plate using silica gel. After coating the temperature sensor with thermal paste, it is inserted into the hole at the center of the heating plate.

The physical diagram of 24 sets of horizontal and vertical compatible diffusion test systems is shown in Fig. 2. Each diffusion test system uses an acrylonitrile butadiene styrene plastic case with a size of 290 × 260 × 80 mm. The aluminum front panel has a power switch and a 3.5-inch touchscreen installed. The upper end of the chassis is a vertical and horizontal diffusion cell-compatible heater with 24 heating slots. It can be placed in 24

horizontal diffusion cells or 24 vertical diffusion cells. The top of the heater covers the transparent acrylic plate insulation cover.

2.2 Structure and Processing of Heating Plate

The multifunctional transdermal diffusion system is classified into four types of heating plates, as shown in Fig. 3. In the figure, (a) is vertical and horizontal compatible with 12 sets of heating plates, (b) is vertical and horizontal compatible with 24 sets of heating plates, (c) is vertical with 24 sets of heating plates, and (d) is vertical with 36 sets of heating plates.

The four types of aluminum heating plates are all 20-mm thick; their dimensions are 192×119, 192×215, 205×151, and 219×219 (unit: mm). The heating plate uses a computer numerical control milling machine to process each groove of the diffusion cell one by one, and then grinds it with a trowel until it becomes smooth. Finally, it is treated with chemical nickel plating to prevent corrosion and oxidation. The nickel plating thickness is 0.1 mm.

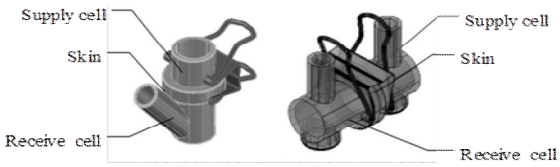

Fig. 4 Diffusion pool structure

2.3 Structure of Processing of Diffusion Cell

As shown in Fig. 4, the vertical and horizontal diffusion cells consist of a supply cell and receiving cell. The horizontal diffusion cell is formed by docking two identical diffusion cells, and the vertical diffusion cell is composed of a receiving cell and supply cell with sampling ports. The volume of the two diffusion tanks is 4.0 mL; the diffusion tank flange diameter is 14 mm, the outer diameter is 24 mm, the effective diffusion area is 147.6 mm2, and sampling port inner diameter is 8 mm; both diffusion cells are fabricated from handmade transparent glass. First, the glass tube with an outer diameter of 14 mm and that with a 10-mm sampling port were cut; then, the flange was processed and connected by flame melting. The flange is finally frosted to a thickness of 3 mm.

3. Principle of Electromagnetic Stirring

To drive the magnetic stirrer to its rotation and speed control, the system uses the rotating magnetic field generated by the iron core coil. The four coils form a group; a pair of coils generate magnetic fields with opposite polarities during operation. The current and magnetic changes in the coils are shown in Fig. 5. One rotation period is divided into steps 1–4. In the first step, the symmetric coils (1 and 3) are turned on; the current directions are opposite, and north (N) and south (S) magnetic poles are generated, respectively. In the second step, coils 2 and 4 are turned on, current directions are opposite,

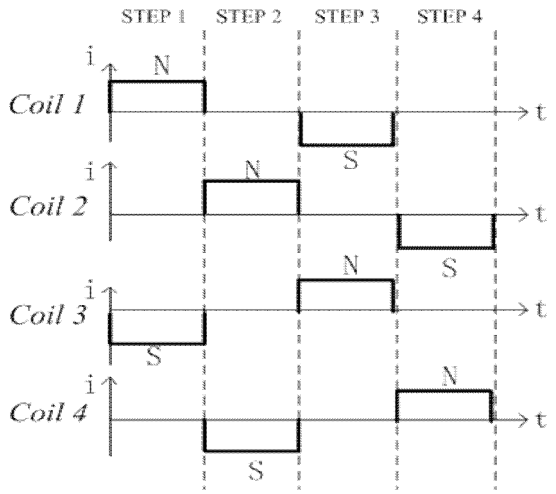

Fig. 5 Coil working waveform

Fig. 6 Physical diagram of coils arrangement

and N and S magnetic poles are generated, respectively. The angles in the first and second steps are 90°. The working principles of the third and fourth steps are the same as the foregoing.

Each system coil presents a rectangular layout. The 12 sets of vertical and horizontal compatible system coils are arranged as shown in Fig. 6. Six coils are placed in the first row, seven coils are placed in the second row, the coils in the third row are aligned with the coils in the first row, and the coils in the fourth row are aligned with the coils in the second row, and so on. The upper, lower, left, and right coils are arranged in a square as a group to drive the rotation of stirrer in the diffusion cell, thus overcoming the unstable actuation of the stirrer jumping around.

Each vertical diffusion cell requires four coils to drive one stirrer. Each horizontal diffusion cell requires six coils to drive two stirrers, of which two coils are shared by the left and right stirrers. In the arrangement, the entire circuit board has 58 coils that can drive 24 stirrers. Each coil has an inner diameter of 4 mm, a height of 10 mm, 220 turns, a wire diameter of 0.3 mm, and a resistance of 1.11 Ω. Each coil is fixed on the circuit board with a galvanized nut and screw with a gasket in the middle.

4. System Hardware and Software

4.1 System Hardware Composition

As shown in Fig. 7, the system hardware is mainly composed of the following: STC15W408AS6 microcontroller unit (MCU), DC48270B43 touchscreen, DS18B20 digital temperature sensor, heating chip drive circuit, coil drive circuit, buzzer, and switching power supply. The coil drive circuit is divided into two groups, which are alternately turned on; each drive circuit is composed of four IRF540 metal–oxide–semiconductor field-effect transistors. The switching power supplies generate 5-V and 36-V DC voltages.

4.2 MCU Interface Circuit

The STC15W408AS MCU is in a 20-pin dual in-line package. The MCU mainly includes an 8-bit CPU, 8k program memory, 512-byte RAM, 5-kB

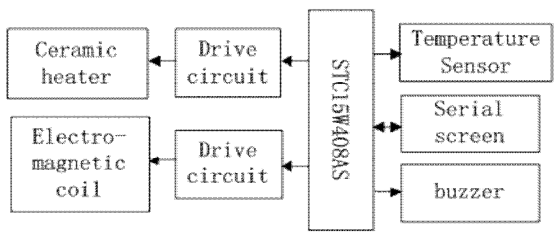

Fig. 7 Hardware composition block diagram

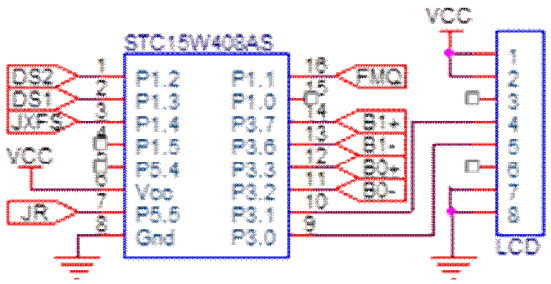

Fig. 8 MCU Interface Circuit

EEPROM, 1 UART, and 3 PWM output port watchdogs. The P3.0 and P3.1 pins of the MCU are connected to the TXD and RXD pins of the DC48270B43 touchscreen, respectively. The baud rate of the serial port is 9600 bps, and DS1 (P1.3) and DS2 (P1.2) are connected to the DS18B20 data line to detect the heater temperature and internal temperature of the chassis, respectively.

The driving triode connects JXFS (P1.4) to the chassis cooling fan, JR (P5.5) is connected to a 150-Ω internal heating plate by IRF540, and different heaters are composed of 4–8 heating sheets in parallel. The FMQ (P1.1) is connected to the ceramic buzzer. The four pins, i.e., B0+(P3.3), B0-(P3.2), B1+(P3.7), and B1-(P3.6), are connected to four coil sets through two INF540s. Each group of coils are connected in series with 14–15 coils and outputs positive and negative alternating square wave pulses to control the coil driving circuit. The MCU interface circuit is shown in Fig. 8.

4.3 System Software

The C51 language is used to the write programs, and KeilμVision5 is the compilation software employed. The system software includes the main function, DS18B20 temperature detection function, timer function, PID algorithm function, touchscreen control function, and buzzer alarm function.

After the start up, the main function is run to display the heater temperature, stirring speed, etc. The heater is regulated to increase the temperature

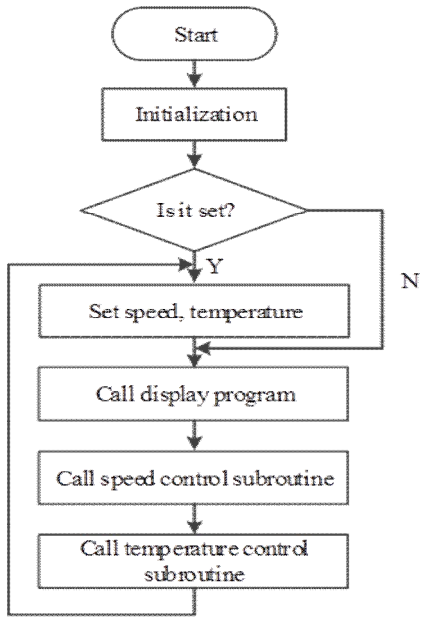

Fig. 9 Program flow chart

to the set temperature, output the coil drive pulse, and wait for the timing to activate the button data. The temperature detection function measures the internal temperature of the heater and cabinet. The flowchart of the main function is shown in Fig. 9.

The temperature control quality of the heater is disturbed by the internal temperature change in the cabinet. Accordingly, the internal temperature in the cabinet is regulated to a certain extent by the cooling fan. The heater temperature is regulated by the PID algorithm, and the amount of output control is calculated based on the set value; the control amount is given by the PWM signal. The temperature sampling period is 1 s, the DA conversion resolution of DS18B20 is 11 bits in binary, and the conversion time is 750 ms.

5. Experimental Result and Analysis

5.1 In Vitro Percutaneous Permeability Test of Bisoprolol Patch

Fig. 10 Experimental physical map

The experiment was commissioned by the School of Pharmacy of Shenyang Pharmaceutical University, using 12 sets of vertical and horizontal compatible transdermal systems, as shown in Fig. 10.

The in vitro percutaneous permeability of bisoprolol patches was investigated using a horizontal diffusion cell. Bisoprolol fumarate (BSP-F) is extracted, separated, filtered, evaporated, and dried; the yellow oily transparent liquid obtained is BSP7. Lauric acid and BSP, which have equal molar numbers, are treated by stirring, rotary evaporation, drying, etc., and the pale yellow waxy solid is obtained as a bisoprolol–lauric acid ion pair (BSP–L)8. The bisoprolol pressure-sensitive adhesive-dispersed patch was prepared by an organic solvent volatilization method. The successfully prepared patch was cut into a pellet-shaped bisoprolol transdermal absorption patch with a diameter of 16 mm. The treated rat skin was frozen for later use.

The stirring speed in the diffusion cell is set to 600 rpm, and the temperature of the receiving liquid is set to 32 °C. After thawing, the rat skin stratum corneum is laid up on the anti-sticking layer, and the prepared bisoprolol transdermal absorption patch is attached to the center of the skin to remove air bubbles between the patch and skin. Then, the skin is fixed on the diffusion cell. The two diffusion cells are placed opposite each other, and the middle cell is fixed by a steel clip9, and 4.0 mL of the receiving solution is added to each diffusion cell; the receiving solution is phosphate buffer (PBS) containing 0.1% NaN3. The stopper is capped. At 2, 4, 6, 8, 10, 12, 24, 28, 32, 36, 48, 52, 56, 60, and 72 h, 2-mL samples were taken from the diffusion cell, whereas an equal volume of fresh 0.1% NaN3 PBS was added to maintain the leakage condition in the receiving solution. The obtained sample was centrifuged at 1 ° C, 16 000 rpm for 7 min, and then appropriately diluted and injected into a high-performance liquid chromatograph for analysis.

5.2 Data Processing

The formula for calculating the cumulative permeation per unit area of bisoprolol in the patch at each sampling time point is as follows:

$$Q = (C_i \times V + \sum_{i=1}^{n-1} C_{i-1} \times V_i / A \quad (1)$$

where Q is the cumulative permeation per unit area, V is the volume of the diffusion cell (4.0 mL), and V_i is the volume of each sample. Ci and C_i−1 are the drug concentrations in the receiving liquid at the i-th and (i−1)th sampling, respectively, and A is the effective diffusion area (1.767 cm^2). The cumulative transmittance per unit area is plotted against time, and the slope of the straight line is the steady state transmittance rate (J·s and S, μ $g/cm^2/h$, respectively). The penetration-promoting ratio (i.e., enhancement ratio) ER is used to evaluate the ability of the promoter to promote drug permeation. The calculation formula is as follows:

$$ER = Q_{72h}(\text{with enhancer}) / Q_{72h}(\text{without enhancer}) \quad (2)$$

where Q_{72h}(with enhancer) and Q_{72h}(without enhancer) are respectively the cumulative permeation amounts of drugs with and without chemical penetration enhancers within 72 h[10~11], respectively. To eliminate individual differences in between the

isolated skin, all experiments are performed 3 to 4 times in parallel; and the results were are shown as mean ± standard error. The statistical analysis method of data adopts variance analysis and t test, with significant difference when P<0.05.

5.3 Experimental Result

The cumulative permeation-time curve of the BSP patch is shown in Fig. 11. The results show that the permeated drug content increases continuously over time; it rises rapidly in the first 30 h and thereafter increases gradually. The cumulative penetration of AZ-added patch at 72 h was 1048.75 ± 61.81 μg/cm2. For the BSP, its transdermal transmission was probably related to the lipophilicity of the penetration enhancer. AZ is highly lipophilic and is easier to diffuse into the lipophilic stratum

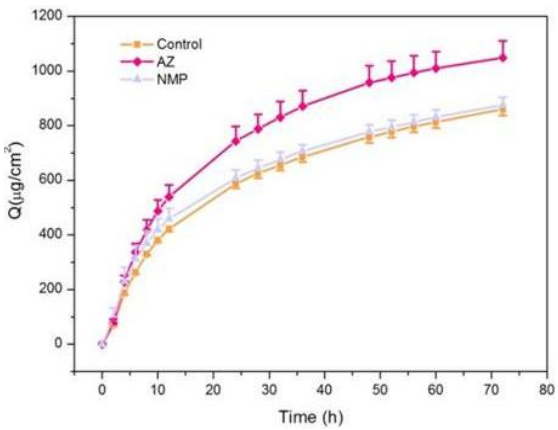

Fig. 11 Percutaneous penetration curve of BSP patch

Table 1 Influence of different chemical penetrating agents on percutaneous Penetration parameters of drugs in BSP patch

Enhancers	Q_{72h}/(μg/cm^2)	ER^a
Control	859.96±22.35	1
AZ	1048.75±61.81	1.22
NMP	875.90±27.88	1.02

Data are given as Mean±SD.(n=3~4)

corneum environment (which acts as the main skin barrier) and changes the lipid regions among the stratum corneum cells, thus promoting the percutaneous transmission of BSP.

6. Conclusion

The multifunctional transdermal diffusion test system achieves system compatibility with horizontal and vertical diffusion cells, increases the number of experiments, and can implement more experimental studies simultaneously; accordingly, it improves the working efficiency. The effects of the diffusion area and sampling port of the diffusion cell are increased. The volume of the diffusion cell is reduced, which is not only convenient for operation but also beneficial for subsequent liquid phase analysis. Electromagnetic stirring replaces the previous method of motor agitation. Its structure is simple, it has a long life, and does not cause wear. The in vitro percutaneous permeability test of the bisoprolol patch verifies the reliability and practicability of the device through the treatment of samples, analysis of derived experimental data, and conduct of numerous experiments.

References

1. Li, Y. W., Liu, W. Z., & Lin, L., “Neuroprotectiv e effects of a GIP analogue in the MPTP Parkinso n’s disease mouse model”, Journal of the Neuropha rmacology, Vol. 63, No. 11, pp. 255-263, 2016.
2. Tian, L, Zhang, S, Lin, H. Q., Deng, H., & Zhang, X. L., “Research progress of transdermal diffusion test methods for transdermal drug delivery”, Chinese Pharmacy, Vol. 23, No. 29 ,pp. 2761-2764, 2012.
3. Wang, Y. Z, Ren, T. C., & Sun, X. M., “Advances in research on oil-water partition coefficient and percutaneous absorption rate

constant of Lappaconitine", Journal of Shandong University of Traditional Chinese Medicine, Vol. 12, No. 02, pp.155-156, 2006.

4. Li, Z. H., Sun, H. Y., Wang, H., Xu, P., & Hou, H. M., "Improvement of in vitro diffusion cell in percutaneous drug administration research", China Pharmaceutical Industry Journal, No. 07, pp. 309-3 10+333. 1995.
5. Keshary, P. R., Chien, Y. W., "Mechanism soft tra nsdermal controlled nitroglycerin administration dev elopment of finite dosing skin permeation system", Vol. 10, No. 06, pp. 883, 2014.
6. Hong Jing Technology Co. Ltd. IAP15W413AS Mi crocontroller Devices Using Manual.
7. BHATT, J., SUBBAIAH, G., &KAMBLI, S., " hig h throughput and sensitive liquid chromatography-ta ndem mass spectrometry method for the estimation of bisoprolol in human plasma using multiplexing t echnique" Journal of Chromatography B, Vol. 852, No. 01, pp. 382-428, 2017.
8. Hefnawy, M. M., Sultan, M. A., Al-Shehri, M. M., "Chemical and Pharmaceutical Bulletin", Public We lfare Corporation Japan Pharmaceutical Society, Vo l. 55, No. 08, pp. 816_2, 2019.
9. Wang, H. Y., Fan, P. F., Zhang, D., "Ultrasound mediated transdermal drug delivery of fluorescent n anoparticles and hyaluronic acid into porcine skin i n vitro", Chinese Physics B, Vol. 25, No. 12, pp. 102-109, 2016.
10. Zhang, J., Du, H. G., Zhang, E. H., Ke, G. M., Wang, L. "Study on the structure characterization a nd transdermal properties of bisoprolol", Journal of Beijing University of Chemical Technology, Vol. 0 4, No. 2, pp. 65-69, 2016.
11. Zhang, X. H., Ouyang, J., & Baeyens, W. R. G., "Enantiomeric separation of β-blockers by HPLC u sing(R)-1-naphthylglycine and 3,5-dinitroben-zoic ac id as chiral stationary phase", Journal of Pharmace utical and Biomedical Analysis, Vol. 23, No. 14, p p. 44, 2013.